

Three-dimensional codes for simulating electron beam transport and free-electron laser operation including space-charge effects

Y. PINHASI†, M. COHEN† and A. GOVER†

Three-dimensional models which describe the electron beam transport and electromagnetic (EM) interaction in a Free-electron laser (FEL) are presented. The models are based on single particle force equations, and take into account emittance and space-charge effects in the e-beam, and transverse spatial variation in the radiation field. In the e-beam transport problem, a cylindrically symmetrical transverse density distribution is assumed, having an arbitrary azimuthal and radial angular spread. The particle trajectories are obtained by solving numerically the equation of motion for a general electric and magnetic field in the presence of space-charge forces. The parameters of the particles in the beam are then displayed in real space and phase space. In the FEL model, the total electromagnetic field (including the RF space-charge field) is expanded in terms of normal modes of the waveguide (including the cut-off modes). The field interaction with the e-beam is described by the force equation for electrons and a set of EM excitation equations for the waveguide modes. The model takes into account 3-D effects of the radiation and space-charge fields, and thus provides a complete description of the FEL interaction for any kind of symmetry of the e-beam and of the waveguide cross-section. The equations are solved numerically to simulate FEL operation in the nonlinear Compton or Raman regimes.

1. Introduction

The paper considers two major problems that appear in free-electron laser (FEL) analysis and design: electron beam transport and electron beam interaction with radiation in the FEL cavity. Two separate codes for simulating these problems have been developed.

For FEL experiments, a low-emittance, high-intensity e-beam is pre-accelerated, bunched, focused, then matched to the main acceleration section in order to inject it into the wiggler (Freund and Antonsen 1992, Goldstein and Newnam 1991, Bengtsson and Kim 1991). The beam quality requirements inside the wiggler are, in general, very stringent. E-beam transport through the low-energy section may spoil beam quality, as evidenced by emittance growth due to space-charge forces and lens aberrations; this limits the gain that can be expected for a given set of parameters. The beam in the low-energy section is typically dominated by space-charge forces. In many cases the beam emittance could play a significant role in the device behaviour. Azimuthal and radial angular momentum spread that are generated close to the entrance plane influence the individual electron trajectories. This effect yields a subsequent current density phase space distribution, which differs from that estimated by models which do not consider these spreads. A model based on particle equations of motion, which are used to derive the particle trajectories for a general field structure. The present treatment considers the problem of a continuous,

Received 6 January 1994; revised 8 July 1994; accepted 12 July 1994.

†Department of Electrical Engineering-Physical Electronics, Tel-Aviv University, Ramat-Aviv, 69978, Israel.

azimuthally symmetrical beam taking into account azimuthal and radial angular momentum spread and space-charged forces. This is an extension of common 2-D models where only the phase space coordinated (r, p_r) are considered. Here we also allow spread in the azimuthal momentum p_θ . A method of treating the space-charge forces for any given particle distribution is introduced. This model permits analysis of a beam with any initial charge distribution and therefore can be used to study the emittance growth problem. The equations of motion are solved and studied numerically.

The 3-D nonlinear FEL code calculates the electromagnetic (EM) field excited by an e-beam drifting along a waveguide in the presence of a wiggler field. Based on the coupled-mode approach presented by Pinhasi *et al.* (1992), the total EM field is expanded in terms of waveguide modes. Such a representation was shown to include the space-charge waves excited in the density modulated e-beam (Pinhasi and Gover 1993). The code solves a set of coupled equations numerically for the amplitude of the excited waveguide modes, together with the single-particle dynamic equations.

2. Dynamics of the particles and e-beam current calculation

The state of particle i is described by a six-component vector, which consists of position coordinates (x_i, y_i, z_i) and a velocity vector v_i . Here (x, y) are the transverse coordinates and z is along the longitudinal axis of propagation. The velocity of each particle in the presence of electric and magnetic fields is found from the force equation

$$\frac{d\mathbf{p}_i}{dt} = -e[\mathbf{E} + \mathbf{v}_i \times \mathbf{B}] \quad (1)$$

where $\mathbf{p}_i = \gamma_i m \mathbf{v}_i$ is the kinetic momentum, and e and m are the electron charge and mass, respectively. The forcing terms on the right-hand side of (1) are the electric field \mathbf{E} and magnetic induction $\mathbf{B} = \mu_0 \mathbf{H}$. These fields represent the total (DC and AC) forces operating on the particle, and also include the self-field due to space-charge. The Lorentz factor γ_i of each particle is found from the equation for the kinetic energy

$$\frac{d\gamma_i}{dt} = -\frac{e}{mc^2} \mathbf{v}_i \cdot \mathbf{E} \quad (2)$$

where c is the velocity of light. The position of the particle is found after integration of the particle velocity.

It is convenient to take z along the axis of propagation as the independent variable, and replace the time derivative $\frac{d}{dt}$ by $v_{zi} \frac{d}{dz}$. This defines a transformation of variables for each particle, which enables the equations of motion to be written in terms of z . The transverse trajectories of the particle are then given by

$$\begin{aligned} \frac{dx_i}{dz} &= \frac{v_{xi}}{v_{zi}} \\ \frac{dy_i}{dz} &= \frac{v_{yi}}{v_{zi}} \end{aligned} \quad (3)$$

The time it takes a particle to arrive at a position z , $t_i(z)$, is a function of the time t_{0i} when the particle entered at $z=0$, and of its longitudinal velocity v_{zi} along the path of motion:

$$t_i(z) = t_{0i} + \int_0^z \frac{1}{v_{zi}(z')} dz' \quad (4)$$

The distribution of the beam current is determined by the position and velocity of the particles. In a steady-state problem, the current density can be represented as a Fourier series in the time domain:

$$J(x, y, z, t) = J_0(x, y, z) + \sum_{n=1}^{\infty} \Re\{\tilde{J}_n(x, y, z) \exp(-jn\omega_s t)\} \quad (5)$$

where ω_s is the fundamental angular frequency of the signal injected into the system. The DC component of the current density is found by averaging the total current over one cycle $T = \frac{2\pi}{\omega_s}$:

$$J_0(x, y, z) = \frac{1}{T} \int_0^T J(x, y, z, t) dt = -\frac{I_0}{N} \sum_{i=1}^N \frac{v_i}{v_{zi}} \delta(x-x_i) \delta(y-y_i) \quad (6)$$

where I_0 is the total current carried by N particles. $\tilde{J}_n(x, y, z)$ is the phasor of the n th harmonic of the current density, and is given by

$$\begin{aligned} \tilde{J}_n(x, y, z) &= \frac{2}{T} \int_0^T J(x, y, z, t) \exp(+jn\omega_s t) dt \\ &= -\frac{2I_0}{N} \sum_{i=1}^N \frac{v_i}{v_{zi}} \delta(x-x_i) \delta(y-y_i) \exp(+jn\omega_s t_i(z)) \end{aligned} \quad (7)$$

The DC current distribution $J_0(x, y, z)$ is used in the transport code to calculate the self space-charge field in the beam. The alternating current components are the ones that excite the RF electromagnetic field.

3. Electron beam transport

3.1. Equations of motion

For the beam transport the problem is solved in a cylindrical coordinate system assuming azimuthal symmetry. Taking the radial component of the force equation (1) yields

$$r'' = -\frac{e}{\gamma m v_z^2} [v_z B_z r \theta' + v_z B_r r r' \theta' - E_z r' + E_r + E_r^b - v_z B_\theta^b] + r \theta'^2 \quad (8)$$

where E_r^b and B_θ^b are the electron space-charge fields, B_z and B_r are the axial and radial components of the focusing magnetic field, and E_z and E_r are the axial and radial components of the electric field. Prime denotes derivatives with respect to z .

The angular velocity is obtained from the conservation of the canonical angular momentum:

$$\theta'(r) = \frac{eB_z(r, z)}{2\gamma mc\beta_z} + \frac{L_{\theta_0}(r_0)}{\gamma mc\beta_z r^2} \quad (9)$$

where $L_{\theta_0}(r_0) = p_{\theta_0}r_0 - eB_{z0}(r_0)r_0^2/2$ is the canonical angular momentum at the entrance plane ($z=0$) and r_0 is the radial distance from the axis where the particle is launched. The axial velocity of the electron is determined from:

$$\beta_z = \left[1 - \frac{1}{\gamma^2} \left(1 + \frac{p_\theta^2 + p_r^2}{m^2 c^2} \right) \right]^{1/2} \quad (10)$$

It is assumed that the electrons in the beam may have non-vanishing initial canonical angular momentum, $L_\theta \neq 0$. Such electrons never cross the beam axis because of the centrifugal force, and they follow non-meridional trajectories in the rotating Larmor reference frame.

Assuming slow variation of the current density in the axial dimension, we use the axial component of Ampere's law and Gauss' law to derive the azimuthal magnetic field and the radial electric field, respectively:

$$\begin{aligned} B_\theta^b(r) &= \frac{\mu_0}{2\pi r} I(r) \\ E_r^b(r) &= \frac{1}{2\pi\epsilon_0 v_z r} I(r) \end{aligned} \quad (11)$$

where $I(r)$ is the current contained within a circle of radius r around the z axis:

$$I(r, z) = 2\pi \int_0^r \xi J_{0z}(\xi, z) d\xi \quad (12)$$

Substituting the angular velocity from (9) and the space-charge fields from (11) into the radial equation of motion (8) gives

$$r'' = - \left[\frac{\Omega_L(r, z)}{c\beta_z} \right]^2 r + \frac{e}{2\gamma mc^2 \beta_z^2} E_r^b r + \left[\frac{L_{\theta_0}}{\gamma mc\beta_z} \right]^2 \frac{1}{r^3} - \frac{K(r)}{r} \quad (13)$$

where $\Omega_L(r, z) = eB_z(r, z)/2\gamma mc\beta_z$ is the Larmor frequency, and $K(r)$ is the radius-dependent beam perveance, defined as

$$K(r) = \frac{e}{\gamma mc^2 \beta_z^2} (E_r^b - v_z B_\theta^b) r = \frac{eI(r)}{2\pi\epsilon_0 \gamma \gamma_z^2 mc^3 \beta_z^3} \quad (14)$$

If the canonical angular momentum term is neglected and a uniform density current at $z=0$ is assumed, and if the profiles of the axial magnetic and electrostatic fields are uniform across the beam, the equation of motion simply includes three linear forces. Particles in a monoenergetic beam, which are launched parallel to the axis, will exhibit a laminar flow (Lawson 1987).

3.2. Electron beam representation

The model can utilize a general circular symmetry e-beam distribution. In the following a gaussian electron beam distribution is investigated. At the entrance plane the beam is assumed to be at its waist, where it is separable in Cartesian coordinates. The problem can be simplified by exploiting the azimuthal symmetry

and representing it in a cylindrical coordinate system, resulting in the normalized distribution function

$$g_0(r, p_r, p_\theta) = \frac{r}{\pi r_b^2 p_b^2} \exp \left[- \left(\frac{r^2}{2r_b^2} + \frac{p_r^2 + p_\theta^2}{p_b^2} \right) \right] \quad (15)$$

For proper sampling, the distribution functions were divided into N equal area segments, where N is the number of macroparticles at a given velocity-space dimension. One macroparticle is placed at the centre of mass of each of the N segments. Each macroparticle represents the same portion of the total current in the beam.

The focusing of an electron beam is studied for a specific example of a shielded solenoid magnetic lens. Its axial magnetic field can be described on the axis by the expression (Loschialpo *et al.* 1985, Ramian and Elias 1987, Cohen and Gover 1993)

$$B(0, z) = B_0 \frac{\exp(-z^2/2b^2)}{1 + z^2/a^2} \quad (16)$$

where a and b are constant coefficients, which are fixed for a given magnetic lens. The radial dependence of the magnetic field was calculated using the standard series expansion of the field in the paraxial approximation up to third order in r (namely, including lens aberrations, which have an important effect on emittance growth).

Equations (2), (13) and (16) are solved numerically to study the effects of angular spread and space-charge forces on e-beam transport.

3.3. Numerical example

A simulation of the e-beam transport along the drift region of the e-gun installed in the Israeli Tandem-FEL project (Cohen *et al.* 1993) is presented. The e-gun injector shown in Fig. 1 consists of an assembly of three coils located along a 50 keV drift tube, in which a 1.5 A beam flows. The particle trajectories of a gaussian profile e-beam with radius $r_b = 5.3$ mm and without initial angular momentum spread are presented in Fig. 2. There are 1600 macroparticles in the simulation. For the sake of clarity, only ten particle trajectories are plotted, which exhibit an almost laminar flow. In the following simulation an e-beam which initially has a gaussian charge

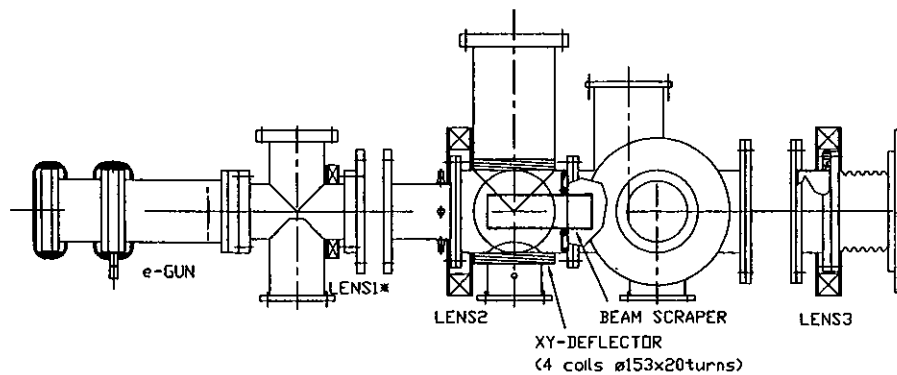


Figure 1. Electron-gun injector of the Israeli Tandem-FEL.

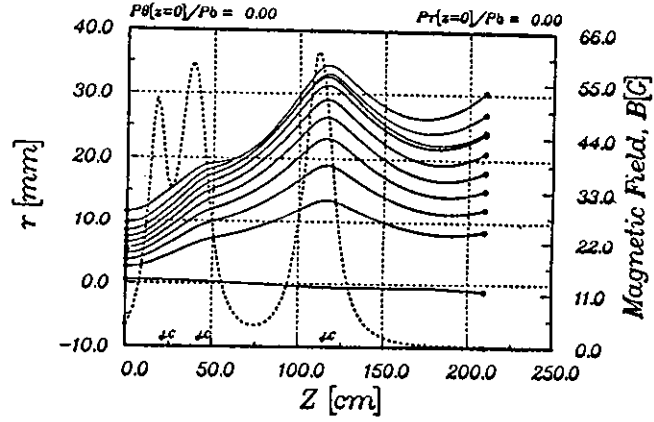


Figure 2. Particle trajectories along the e-gun injector with no initial angular spread.

distribution with or without gaussian angular spread is considered. The normalized emittance of the hot beam is taken to be $\varepsilon_n = 100\pi$ mm mrad.

Figure 3 depicts the evolution of a projected 2-D phase space at five points along the axis. In the phase space plots the coordinates (x, x') stand for each particle trajectory in a given axial position. In all cases aberration terms are included. Only a small part of the total number of macroparticles that were included in the simulation are presented.

4. FEL code

The mutual interaction between the e-beam and the RF field in a FEL is fully described by the beam dynamics equations (1) and (2) together with the excitation equations of the EM field. Instead of solving the inhomogeneous, steady-state Maxwell vector field equations, we utilize representations of field variables in terms of a complete set of vector eigenfunctions (Marcuvitz and Schwinger 1951, Vaynshtain 1957, Felsen and Marcuvitz 1973). The expansion leads to a set of coupled-mode equations which describe the evolution of the mode amplitudes. These scalar equations are solved self-consistently with the equation of motion of the particles.

4.1. Excitation of the EM field

The total EM field, excited by a harmonic current source $\mathbf{J}(\mathbf{r}, t) = \Re\{\tilde{\mathbf{J}}(\mathbf{r}) \exp(-j\omega_s t)\}$ distributed along the waveguide, is calculated by presenting the transverse components as a superposition of the complete set of TE and TM waveguide modes:

$$\begin{aligned}\tilde{\mathbf{E}}_{\perp}(x, y, z) &= \sum_q C_{+q}(z) \tilde{\mathcal{E}}_{+q\perp}(x, y) \exp(+jk_{zq}z) + C_{-q}(z) \tilde{\mathcal{E}}_{-q\perp}(x, y) \exp(-jk_{zq}z) \\ \tilde{\mathbf{H}}_{\perp}(x, y, z) &= \sum_q C_{+q}(z) \tilde{\mathcal{H}}_{+q\perp}(x, y) \exp(+jk_{zq}z) + C_{-q}(z) \tilde{\mathcal{H}}_{-q\perp}(x, y) \exp(-jk_{zq}z)\end{aligned}\quad (17)$$

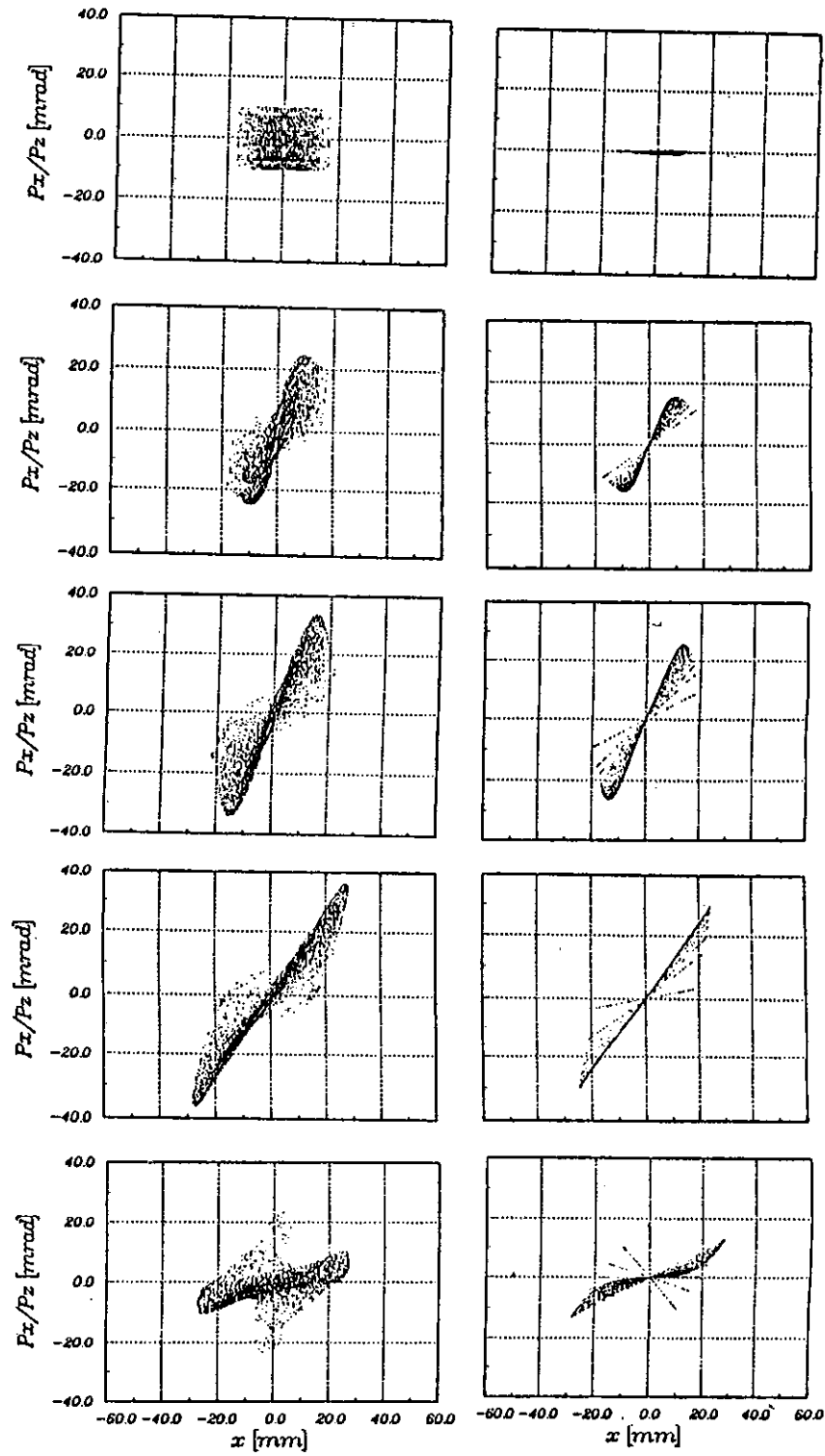


Figure 3. Phase space evolution along the e-gun injector: right column, no initial angular spread in the beam; left column, initial emittance $\varepsilon_n = 100\pi$ mm mrad.

$C_q(z)$ is the slowly-varying amplitude, and $\tilde{\mathcal{E}}_{q\perp}(x, y)$ and $\tilde{\mathcal{H}}_{q\perp}(x, y)$ are complex vectors representing the electric and magnetic transverse field profile and polarization of waveguide mode q . k_{zq} is the longitudinal wavenumber of the mode. The summation includes both propagating and cut-off mode of the waveguide. The expression for the longitudinal component of the EM field is obtained after substitution of the above expansion into the excited Maxwell equations:

$$\begin{aligned}\tilde{E}_z(x, y, z) &= \sum_q C_{+q}(z) \tilde{\mathcal{E}}_{+qz}(x, y) \exp(+jk_{zq}z) + C_{-q}(z) \tilde{\mathcal{E}}_{-qz}(x, y) \exp(-jk_{zq}z) \\ &\quad + \frac{1}{j\omega\epsilon} \tilde{J}_z(x, y, z) \\ \tilde{H}_z(x, y, z) &= \sum_q C_{+q}(z) \tilde{\mathcal{H}}_{+qz}(x, y) \exp(+jk_{zq}z) + C_{-q}(z) \tilde{\mathcal{H}}_{-qz}(x, y) \exp(-jk_{zq}z) \quad (18)\end{aligned}$$

Note that the expression for the longitudinal electric field $\tilde{E}_z(x, y, z)$ includes the plasma wave field excited by the longitudinal space-charge density modulation along the interaction region (Pinhasi and Gover 1993).

From Maxwell's equations, imposing the boundary conditions on the waveguide walls, the evolution of the mode amplitude is found to be described by two scalar differential equations for the forward (+ q) mode

$$\begin{aligned}\frac{d}{dz} C_{+q}(z) &= -\frac{1}{2\mathcal{S}_q} \exp(-jk_{zq}z) \iint \left[\frac{Z_q}{Z_q^*} \tilde{J}_1(x, y, z) + \hat{z} \tilde{J}_z(x, y, z) \right] \cdot \tilde{\mathcal{E}}_{+q}^*(x, y) dx dy \\ &= +\frac{1}{\mathcal{S}_q} \exp(-jk_{zq}z) \frac{I_0}{N} \sum_{i=1}^N \frac{1}{v_{zi}} \left[\frac{Z_q}{Z_q^*} v_{\perp i} + \hat{z} v_{zi} \right] \cdot \tilde{\mathcal{E}}_{+q}^*(x_i, y_i) \exp(+j\omega_s t_i(z))\end{aligned} \quad (19)$$

and the backward (- q) mode

$$\begin{aligned}\frac{d}{dz} C_{-q}(z) &= +\frac{1}{2\mathcal{S}_q} \exp(+jk_{zq}z) \iint \left[\frac{Z_q}{Z_q^*} \tilde{J}_1(x, y, z) + \hat{z} \tilde{J}_z(x, y, z) \right] \cdot \tilde{\mathcal{E}}_{-q}^*(x, y) dx dy \\ &= +\frac{1}{\mathcal{S}_q} \exp(+jk_{zq}z) \frac{I_0}{N} \sum_{i=1}^N \frac{1}{v_{zi}} \left[\frac{Z_q}{Z_q^*} v_{\perp i} + \hat{z} v_{zi} \right] \cdot \tilde{\mathcal{E}}_{-q}^*(x_i, y_i) \exp(+j\omega_s t_i(z))\end{aligned} \quad (20)$$

where Z_q is the mode impedance given by $Z_{TEq} = \frac{\omega_s \mu}{k_{zq}}$ for the TE mode, and $Z_{TMq} = \frac{k_{zq}}{\omega_s \epsilon}$ for the TM mode. The normalized complex power of the mode is

$$\mathcal{S}_q = \iint_{c.s.} [\tilde{\mathcal{E}}_{1q} \times \tilde{\mathcal{H}}_{1q}^*] \cdot \hat{z} dx dy \quad (21)$$

4.2. Numerical results

The numerical simulation presented here is from the millimetre wave Tandem FEM project, which is being developed in Israel by Cohen *et al.* (1993). This free-electron maser (FEM) is based on a 2-6 MeV Tandem Van de Graaff electrostatic accelerator for a 1 A e-beam, and utilizes a magnetostatic planar wiggler with 20 periods of $\lambda_w = 4.4$ cm.

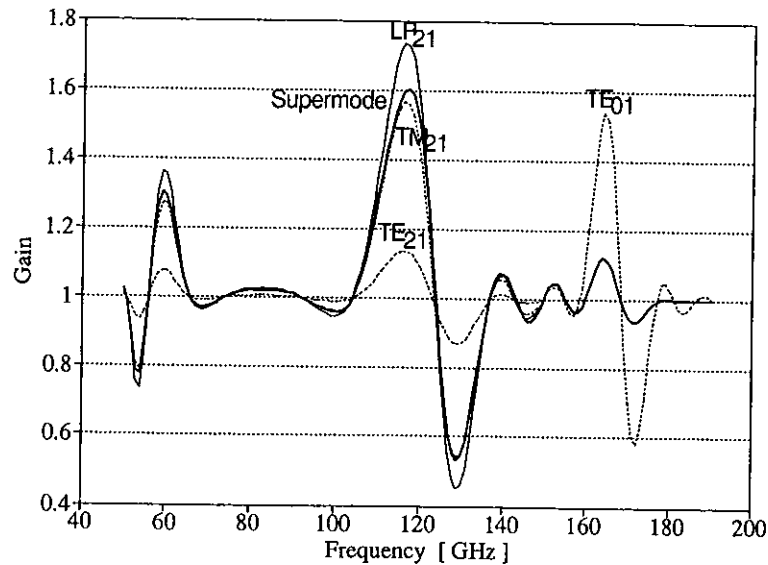


Figure 4. Small-signal gain versus frequency calculated in a multimode simulation.

The RF cavity considered in the simulation is an overmoded $1.5 \times 1.5 \text{ cm}^2$ rectangular waveguide. For the parameters listed above, it is found that the waveguide modes TE_{01} , TE_{21} and TM_{21} interact efficiently with the e-beam. Other non-synchronous modes which do not contribute to the FEL interaction, however, need to be taken into account in order to calculate the space-charge field. Since the transverse modes TE_{21} and TM_{21} are degenerate in their longitudinal wave number k_z , they will operate at the same frequency and may be excited simultaneously. Consequently, the appropriate linear combination of these modes can be calculated to find the normal mode of the FEL system (Pinhasi *et al.* 1992). Such a 'supermode' is characterized by the feature that its field profile and polarization do not change along the interaction region. Note that in the case when the e-beam width is narrow relative to the profiles of the modes, the linearly-polarized mode LP_{21} of the waveguide is exactly the supermode of the FEL.

Figure 4 illustrates the small-signal gain of the FEM as a function of the operating frequency. Single mode gain curves of the TE_{01} , TE_{21} and TM_{21} waveguide modes are given in dashed lines. The solid line describes the small-signal gain obtained from multimode FEL simulation, taking into account the fundamental TE_{01} mode and the linearly polarized LP_{21} mode. The results obtained from the 3-D FEL code agree well with the results calculated analytically from the linear coupled-mode model (Pinhasi *et al.* 1992).

REFERENCES

- BENGTSSON, J., and KIM, K. J., 1991, Achromatic and isochronous electron beam transport for tunable free electron lasers. *Nuclear Instrumentation and Methods*, **318**, 344-348.
- COHEN, M., DRAZNIN, M., EICHENBAUM, A., GOLDRING, A., GOVER, A., PINHASI, Y., WACHTEL, J., YAKOVER, Y., SOKOLOWSKI, J., MANDELBAUM, B., ROSENBERG, A., SHILOH, Y., HAZAK, G., LEVINE, M., and SHAHAL, O., 1993, *15th International FEL Conference*, The Hague, The Netherlands (Israeli tandem electrostatic accelerator FEL-status-report, A341, ABS57-ABS58).

- COHEN, M., and GOVER, A., 1993, Effects of azimuthal and radial angular spread on e-beam focusing characteristics in the presence of space-charge forces. *SPIE Proceedings of the Conference on Electron-Beam Sources of High-Brightness Radiation*, San Diego, California, **SPIE 2013**, pp. 24-42.
- FELSEN, L. B., and MARCUVITZ, N., 1973, *Radiation and Scattering of Waves* (Englewood Cliffs, NJ: Prentice Hall).
- FREUND, H. P., and ANTONSEN, T. M., 1992, *Principles of Free Electron Lasers* (New York: Macmillan).
- GOLDSTEIN, J. C., and NEWNAM, B. E., 1991, Injector and accelerator technology. *Nuclear Instrumentation and Methods*, **A318**, 349-476.
- LAWSON, J. D., 1987, *The Physics of Charged-Particle Beams* (Oxford, U.K.: Clarendon Press), Chap. 3.
- LOSCHIALPO, P., NAMKUNG, W., REISER, M., and LAWSON, J. D., 1985, Effects of space charge and lens aberrations in the focusing of an electron beam by a solenoid lens. *Journal of Applied Physics*, **57**, 10-17.
- MARCUVITZ, N., and SCHWINGER, J., 1951, On the representation of the electric and magnetic fields produced by currents and discontinuities in waveguides. *Journal of Applied Physics*, **22**, 806-819.
- PINHASI, Y., and GOVER, A., 1993, Coupled-mode theory of Langmuir space-charge waves for general electron-beam and waveguide cross sections. *Physics Review E*, **48**, 3925-3929.
- PINHASI, Y., GOVER, A., BEST, R. W. B., and VAN DER WIEL, M. J., 1992, Transverse mode excitation and coupling in a waveguide free electron laser. *Nuclear Instrumentation and Methods*, **A318**, 523-527.
- RAMIAN, G., and ELIAS, K., 1987, High-current beam transport in electrostatic accelerator tubes. *Proceedings of the Institute of Electrical and Electronics Engineers*, **58**, 476-481.
- VAYNSHTAIN, L. A., 1957, *Electromagnetic Waves* (Moscow: Sovetskoye Radio).